ACSNANO

www.acsnano.org

ARTICLE

Nanoscopic Terraces, Mesas, and Ridges in Freely Standing Thin Films Sculpted by Supramolecular Oscillatory Surface Forces

Yiran Zhang, Subinuer Yilixiati, Collin Pearsall, and Vivek Sharma*

Department of Chemical Engineering, University of Illinois at Chicago, Chicago, Illinois 60607, United States

Supporting Information

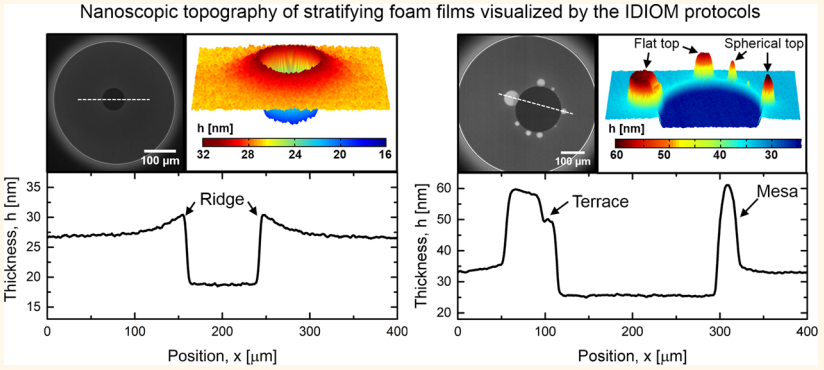

ABSTRACT: **Freely standing thin liquid films containing supramolecular structures including micelles, nanoparticles, polyelectrolyte−surfactant complexes, and smectic liquid crystals undergo drainage via stratification. The layer-by-layer removal of these supramolecular structures manifests as stepwise thinning over time and a coexistence of domains and nanostructures of discretely different thickness. The layering of supramolecular structures in confined thin films contributes additional non-DLVO, supramolecular oscillatory surface forces to disjoining pressure, thus influencing both drainage kinetics and stability of thin films. Understanding and characterizing the spontaneous creation and evolution of nanoscopic topography of stratifying, freely standing thin liquid films have been long-standing challenges due to the absence of experimental techniques with the requisite spatial (thickness <10 nm) and temporal resolution (<1 ms). Using Interferometry Digital Imaging Optical Microscopy (IDIOM) protocols developed herein, we visualize and characterize size, shape, and evolution kinetics of nanoscopic mesas, terraces, and ridges. The exquisite thickness maps created using IDIOM protocols provide much needed and unprecedented insights into the role of supramolecular oscillatory surface forces in driving growth of such nanostructures as well as in controlling properties and stability of freely standing thin films and, more generally, of colloidal dispersions like foams.**

KEYWORDS: *thin film, imaging, optical microscopy, micelles, surface forces, DLVO theory*

Visualizing, characterizing, and understanding the spontaneous creation and evolution of nanoscopic topography of freely standing thin liquid films have been long-standing challenges due to the absence of experimental techniques with the requisite spatial (thickness <10 nm) and temporal resolution (<1 ms). In contrast, significant progress in understanding of the structure and stability of supported thin films[1−8] (with at least one solid/liquid interface) has occurred through the emergence and advances in several microscopy and force-based experimental techniques[1−4] including surface force apparatus (SFA), fluorescence imaging, atomic force microscopy (AFM), total internal reflection microscopy (TIRM), ellipsometry, and electron microscopy. The stability and properties of supported thin films are of critical importance for coatings and thin-film technologies[3−6] as well as stability, rheology, and applications of colloidal nanoparticle dispersions.[1,9,10] Correspondingly, the forces and flows that drive drainage and rupture of individual freely standing films determine stability and physiochemical properties of soap bubbles, cell membranes, and colloidal dispersions like emulsions and foams with drops or gas pockets, respectively, as the dispersed phase.[9,11,12] We show that using a combination of interferometry, digital imaging, and optical microscopy, referred hereafter as IDIOM protocols, provide the requisite spatial-temporal resolution for noninvasively imaging

Received: February 9, 2016
Accepted: April 8, 2016

DOI: 10.1021/acsnano.6b01012
ACS Nano XXXX, XXX, XXX−XXX

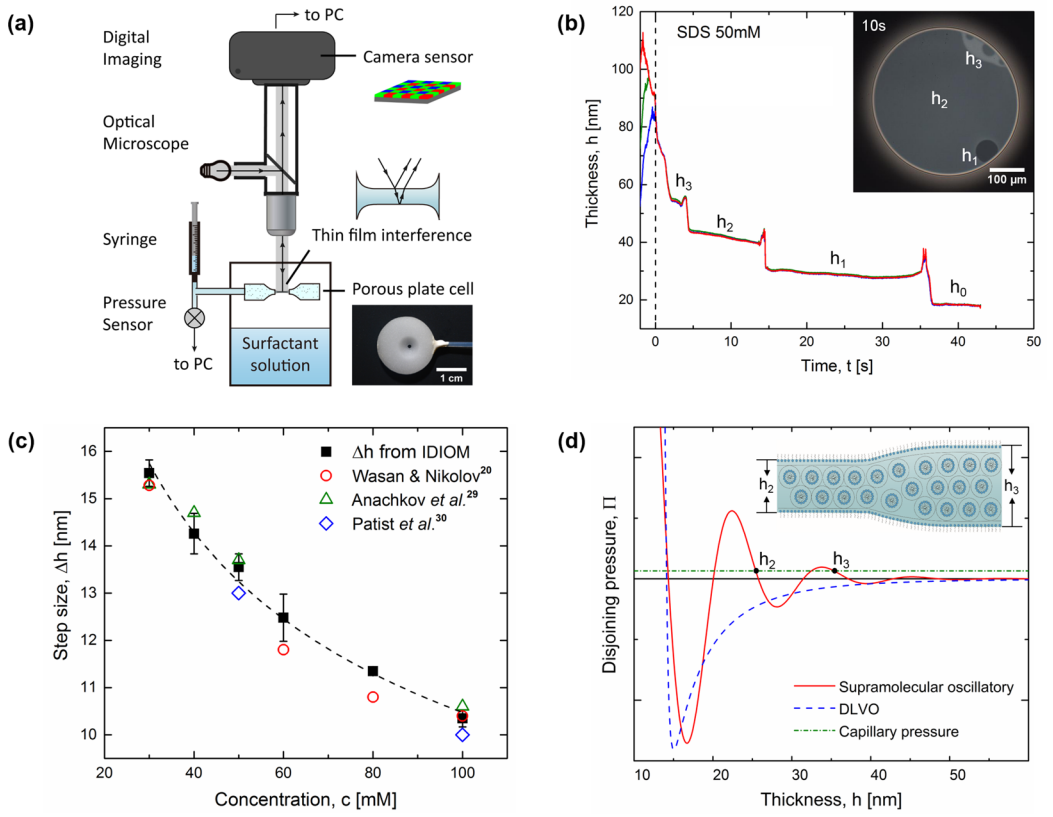

Figure 1. Drainage and stratification in micellar foam film. (a) Schematic of the experimental setup used for determining thin-film thickness $h(x,y,t)$ using a combination of interferometry, digital imaging, and optical microscopy (IDIOM). The digital imaging algorithm includes detection of spatial variation in interference intensity $I(x,y,t)$ at each pixel using camera sensor array, and using digital filtering allows access to three distinct intensity maps corresponding to red, green, and blue channels. (b). The mean thickness is computed from intensity averaged over a 20 μm region at the center of the horizontal foam film made from SDS solution (c = 50 mM solution, c_{CMC} = 8.2 mM). The time t = 0 corresponds to the instant when the last interference maxima is reached for the shortest wavelength. The micrograph at t = 10 s, included as an inset, shows three distinct shades of gray, implying regions of different thickness coexist. (c) Concentration-dependent variation in step size $\Delta h = h_{n+1} - h_n$ obtained using the IDIOM method compares well with the values obtained with the conventional interferometry measurements[20,29] and theoretical estimates.[30] The dashed line shows the scaling law $\Delta h \propto c^{-1/3}$ characteristic of packed spheres. (d) Contributions to the disjoining pressure in 80 mM SDS thin film are shown. The DLVO contributions calculated using $\Pi_{DLVO}(h) = \Pi_{vdW}(h) + \Pi_{el}(h)$ decay at a thickness of 30 nm, while the supramolecular oscillatory contributions to disjoining pressure are longer ranged.

and characterizing the evolution of structure, dynamics, and topography of freely standing thin films. Using IDIOM protocols, we visualize distinct geometrical features like terraces, mesas, craters, and ridges, both flat and nonflat nanostructures, within freely standing thin films.

The study of freely standing films or soap films and "soap bubbles, their colors, and the forces that mold them,"[13] as well as the their stability and lifetime, has forever fascinated scientists and nonscientists alike.[12−15] For films with thickness approaching molecular length scale, intermolecular and surface forces contribute a thickness-dependent excess pressure called disjoining pressure $\Pi(h)$ that can counterbalance capillary pressure that drives drainage within foam films.[10,16] The strength of capillary pressure, and counteracting bulk and interfacial stresses, depends upon the physicochemical properties of the amphiphilic molecules that spontaneously adsorb at the liquid/air interface.[9−17] Dispersion forces (van der Waals attraction) $\Pi_{vdW}(h)$ and repulsive electrostatic double-layer forces $\Pi_{el}(h)$ together provide a simple and useful estimate for disjoining pressure[1,10,16] and form a basis of the DLVO theory for colloidal stability.[1,9,16] Typically drainage in foam films is characterized by a monotonic decrease in thickness, culminating in formation of common black films (typically 10 < h < 30 nm) as eventually disjoining pressure and capillary pressure balance each other.[12,14−17] However, foam films containing supramolecular structures including micelles, bilayers, nanoparticles, smectic liquid crystals, and polyelectrolytes[18−24] undergo stratification, *i.e.*, exhibit stepwise thinning over time, and during drainage, thin films show coexistence of domains and nanostructures of discretely different thickness (see Figure 1). Stratification in these confined fluids is caused by layering of supramolecular structures,[19,21,22] which results in additional non-DLVO, supramolecular oscillatory surface force contributions $\Pi_{os}(h)$ to disjoining pressure (see Supporting Information). We show that Interferometry Digital Imaging Optical Microscopy (IDIOM) protocols developed herein provide unprecedented spatial (thickness <10 nm) and temporal resolution (<1 ms) for visualization and analysis of the stratification process and the nanostructures sculpted by supramolecular, non-DLVO forces. The thickness maps provide critical insights into the role of supramolecular oscillatory surface forces in driving growth of such nanostructures as well as in controlling properties and stability of thin films and, more generally, of colloidal dispersions like foams.

DOI: 10.1021/acsnano.6b01012
ACS Nano XXXX, XXX, XXX−XXX

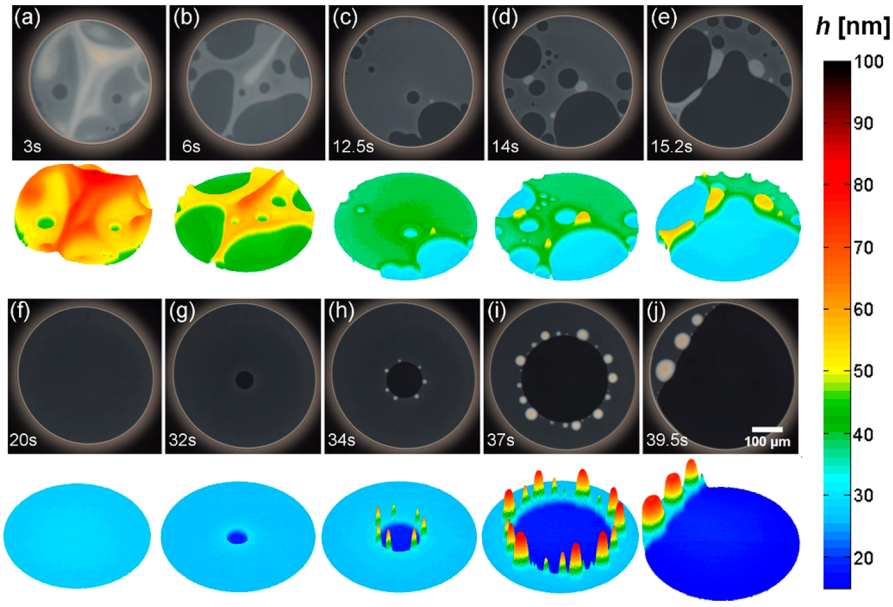

Figure 2. Soapy shades of gray characteristic of stratification process and the height maps obtained using IDIOM methodology highlighting the associated topographical changes. Coexistence of domains of multiple thicknesses and complex transition dynamics from thicker to thinner layers are visualized. (Video, included as Supporting Information, shows a movie compiled from RAW images captured using Photron Fastcam UX100 with Navitar Zoom 6000 magnification system and the corresponding 3D thickness map for the entire stratification process.) The landscape contains nanoscopic mesas, ridges, terraces, and craters. The height varies between 1 and 100 nm, while the in-plane scale bar shows domains are 1−1000 μm, implying that the nanoscopic features have a low aspect ratio.

RESULTS AND DISCUSSION

In the conventional interferometry methods, thickness is computed using light intensity reflected from a spot size of 30−60 μm using a photodetector and a monochromatic light source.[11,25−28] In contrast, the IDIOM protocols described herewith use a white light source and rely on the high-quality CMOS or CCD sensors of digital cameras for capturing a pixel-wise, spatially resolved map of reflected light intensity, $I(x,y,t)$ for each wavelength and for each snapshot. Freshly formed foam films illuminated by white light exhibit multicolored iridescent patterns that arise due to interference between light rays reflected from two liquid/gas interfaces and evolve as thickness variations are produced and advected within these films.[12−15] Though interference colors are visible for thicker films ($h > \lambda/2\pi$), intensity modulated by interference provides a measure of film thickness even for black films that are only a few molecular-layers thick. Following Scheludko,[28] a relatively accurate measure of thickness, h can be obtained by using the following equation based on a normalized measure of intensity, $\Delta = (I - I_{min})/(I_{max} - I_{min})$ that minimizes the influence of source intensity and background/detector errors:

$$h = \left(\frac{\lambda}{2\pi n}\right)\arcsin\left(\sqrt{\frac{\Delta}{1 + 4R(1-\Delta)/(1-R)^2}}\right) \quad (1)$$

Here I_{max} and I_{min}, respectively, correspond to the maximum and minimum values of intensity, and $R = (n-1)^2/(n+1)^2$, the Fresnel coefficient is computed using the value of refractive index, n of the bulk solution (here $n = 1.33$), which provides us a measure of "equivalent film thickness". Eq 1 neglects absorption, includes multiple reflections within the film, assumes a near-normal incidence, and considers only zeroth order of interference; valid assumptions for films with thickness $h < \lambda/2\pi$ (nominally $h < 100$ nm).

The photocurrent incident on the sensor array of the digital camera is converted into RGB intensity values assigned to each pixel in the color image. In the IDIOM method, we digitally filter and split the image into three intensity values corresponding to R (red, λ = 650 nm), G (green, λ = 546 nm), and B (blue, λ = 470 nm) illumination, and using eq 1 obtain three simultaneous measurements of thickness at each pixel.[31] By using a 12-bit sensor and unprocessed, uncompressed images data in RAW format, we infer that the spatial variation in thickness, $h(x,y,t)$ can be resolved with an in-plane (x, y) spatial resolution of ~0.5 μm/pixel, subnanometer out-of-plane (z) resolution, and submillisecond time resolution. The spatiotemporal resolution is limited by the constraints imposed by optical microscopy and the choice of camera sensor/optics (see Supporting Information). While the interferometry protocols have been used for more than a century for foam film studies,[28,32] and many recent studies utilize digital cameras as photometers, spectrophotometers or photodiodes for applications ranging from star-gazing to photoscopy to analyzing structural colors in jewel beetles[33,34] (see Supporting Information), we believe this is the first report of nanoscopic topographical mapping in freely standing films. We first compare the thickness evolution (Figure 1) computed with IDIOM protocols applied to fixed spot of size 20 μm with the conventional interferometry analysis (approach we used in our studies of domain expansion dynamics).[31] We then proceed to provide topographical maps (Figures 2 and 3) showcasing how the IDIOM protocols provide glimpse into structure and dynamics of nanostructures never imaged and analyzed before.

As the detected reflected light intensity $I(x,y,t)$ for any wavelength, λ is modulated by thickness-dependent $h(x,y,t)$ thin-film interference, these stratified films (h < 100 nm) exhibit complex patterns with multiple shades of gray (Figures 1−3). The progressive thinning of thin foam films formed from an aqueous sodium dodecyl sulfate or SDS solution (c = 50

DOI: 10.1021/acsnano.6b01012
ACS Nano XXXX, XXX, XXX−XXX

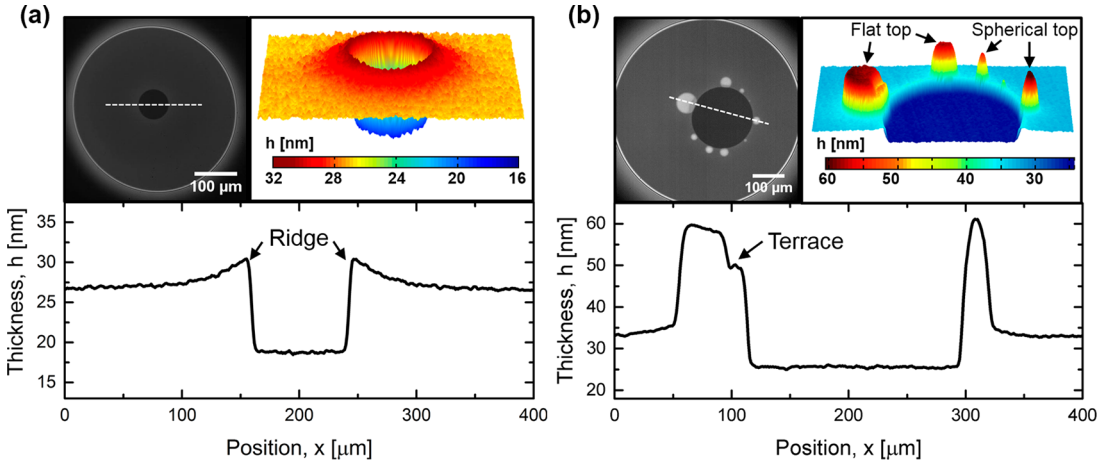

Figure 3. Nanoscopic structures include ridges, mesas, and terraces visualized and analyzed by the IDIOM protocols. Here the height coordinate is in nm range, while the in-plane coordinate is in 100 μm range, implying mesas and ridges are low-aspect ratio structures. (a) Cross-sectional profile of the foam film shows a ridge or a rim adjacent to the growing thinner domain that is several nanometers thicker than the surrounding film. Inset shows a three-dimensional thickness map wherein domain and flanking rim appear to resemble a crater. (b) Profile of the foam film with 80 mM SDS at t = 35.6s shows mesa formation, both flat top and nonflat top mesas as well as a terrace are shown. The mesas are attached to the growing domain and are much thicker than the rest of the film.

mM; c/CMC $\approx$ 6) in a porous plate cell under a capillary pressure $P_c \sim$ 130 Pa, is shown in Figure 1. The height evolution displays several discontinuous jumps or steps, and the height of each step is found to be constant with Δh = 13.5 $\pm$ 0.3 nm. The step-size (Δh) (see Figure 1c) decreases with an increase in concentration, and the values extracted from the IDIOM protocol are similar to those reported in the literature.[20,21,29,30,35] Anachkov et al.[29] posited that the change in step size with concentration of micellar solutions can be analyzed to determine micelle size, aggregation number, and charge, and we have verified that IDIOM protocols provide measures comparable to values obtained in spectroscopic and scattering studies.[29] A simultaneous observation of nanoscopic structures that emerge during stratification shows that the thickness jumps are directly correlated with the lateral motion of thicker or thinner regions into the fixed spot of 20 μm used for intensity and thickness measurement.

Innumerable scientists, including Newton, Hooke, Brewster, Raman, Perrin, Mysels, and deGennes discussed patterns and colors in soap films, including black domains that can spontaneously emerge within soap films drained to nanoscopic thicknesses (h < 40 nm).[12−15] However, Johonnott (1906) was the first to discuss stratification and employ interferometry to study stratified soap films.[32] Thereafter, Perrin examined stratified soap films[36] and included stratification as an evidence for molecular reality, and discontinuous and periodic structure of matter, in his Nobel lecture in 1926. Decades later, stratification was observed and characterized in smectic liquid crystal mesophases[23,24,37−39] (see Oswald and Pieranski[23] for a comprehensive review). Interest in stratifying foam films (with no liquid crystalline mesophases present) reemerged due to a series of papers by Nikolov, Wasan, Kralchevsky, and collaborators in the late 1980s.[18−21] The understanding that ordering induced by confining supramolecular structures like micelles, nanoparticles, and polyelectrolyte−surfactant complexes causes stratification in foam films is fairly recent,[18−22] and most of the studies so far have focused on characterizing thickness evolution and thickness jumps, emulated by data shown in Figure 1. However, the formation and evolution of nanoscopic structures that accompany stratification process have not received sufficient attention, as none of the existing techniques provide suitable spatiotemporal resolution for imaging topography of freely standing films. Using IDIOM protocols, we obtain the first time-resolved visualization of rich and complex topography present in stratifying foam films, and illustrative images and corresponding thickness maps are shown in Figures 2−3 (see video, included as Supporting Information).

Stratification occurs by the formation and expansion of one or more thinner domains that grow at the expense of thicker surrounding films (see Figure 2).[17−23,31,40,41] As domains expand, they coalesce with each other or with the plateau border (see Figure 2b−e). In some instances, the growing domains appear to be flanked by a brighter halo, inferred to be due to the presence of a ridge or a rim, formed by the accumulation of fluid removed from the growth of thinner domain.[40,41] Due to a topological instability, ridges sometimes evolve into one or more white spots or mesas (Figure 2d,e,h−j) that have been called lenses, pancakes, droplets, and globules in literature.[12,17,41] Before the development of IDIOM protocols, no experimental technique possessed temporal and spatial resolution for analyzing such morphological evolution accompanying such topological instabilities and for understanding dynamical processes like nucleation or coalescence of domains or mesas. The IDIOM protocols not only allow access to the shape, size, and growth kinetics of ridges, thinner domains, and mesas but also enable us to probe and address several unanswered questions regarding hydrodynamics of thin freely standing films and the influence of intermolecular and surface forces.[1−8,17−22,26,27,31]

For example, the asymmetrical shape of ridge formed at the periphery of growing domain in stratifying foam films can be henceforth visualized using IDIOM protocols (see Figure 3). The shape of this ridge is similar to that of rim formed near retracting contact line during dewetting of supported ultrathin polymer films.[4,7,8,31] Both ridges and mesas are relatively low aspect ratio structures (height in nm, width in microns), and their shape and shape evolution involve interplay of contributions from oscillatory thickness-dependent disjoining pressure and curvature-dependent Laplace pressure. It is well

DOI: 10.1021/acsnano.6b01012
ACS Nano XXXX, XXX, XXX−XXX

established that a disjoining pressure that includes attractive dispersion and an exponentially decaying repulsion contributions modulates flows and fluxes in supported thin films undergoing dewetting[3,4,8] and leads to formation of black spots in soap films.[25] Correspondingly, for stratifying micellar foam films, since the disjoining pressure includes a longer-ranged supramolecular oscillatory structural force contribution, stratification occurs, and the intermicellar distance (which sets the step size) corresponds to the periodicity of oscillatory forces (see Figure 1 and Supporting Information). While terraced nanostructures occur also in confined simple fluids (characterized by ellipsometry)[7] and smectic liquid crystals,[23,24] appearance of mesas, including terraced mesas with flat tops, is a peculiar feature of these stratifying foam films containing micelles. A detailed analysis of shape evolution of rim as well as of mesas is underway, and our investigations suggest that including the supramolecular oscillatory force contributions in driving pressure term in the thin-film equation captures their characteristic growth dynamics.

CONCLUSIONS

In summary, we show that a combination of interferometry, digital imaging, and optical microscopy (or IDIOM protocols) can be used for visualizing and characterizing thickness variation and topological transitions in freely standing thin films with unprecedented spatial (thickness, z-direction <10 nm; in-plane, $x-y < 1$ μm) and temporal resolution (<1 ms). In this study, we focus on drainage and stratification in micellar foam films formed from aqueous solutions of sodium dodecyl sulfate, with the surfactant present at the fluid/fluid interfaces as well as in bulk as self-assembled supramolecular structures called micelles. Using IDIOM protocols, we visualize and analyze several characteristic features of stratification including discrete changes in thickness, coexistence of regions with different nanoscopic thickness, growth of thinner (darker) domains, and topological transitions that create nonflat structures like ridges and mesas. We believe that the noninvasive imaging and characterization of ridges, mesas, and terraces in freely standing thin films will revolutionize the study of nanoscale rheology and of surface and intermolecular forces, especially the understanding of non-DLVO, supramolecular oscillatory surface forces that underlie stratification. We hope that a widespread use of IDIOM protocols will lead to a better understanding of interactions, flows, and self-assembly in biology, in chemical physics, and in foams and other colloidal systems.

MATERIALS AND METHODS

Materials: Aqueous Solutions of Sodium Dodecyl Sulfate. An anionic surfactant sodium dodecyl sulfate or SDS (molecular weigh of 288 Da, Sigma-Aldrich Co., St. Louis, MO, L6026, >99.0%) is used as-received without further purification to prepare aqueous solutions with deionized water (with resistivity of 18.2 MΩ). Horizontal foam films formed with aqueous SDS solution, with concentrations both below and above the critical micelle concentration (CMC) (literature values range between 7 and 10 mM at 25 °C).[42] It is well-known that the presence of impurities or the presence of trace amounts of 1-dodecanol affect micellization, surface tension, and interfacial rheology.[43,44] The concentration-dependent surface tension of aqueous SDS solutions measured using a maximum bubble pressure tensiometer shows a smooth transition near a CMC value of c = 8.2 mM, indicating that the as-made solutions are relatively free of impurities.[43,44] No electrolytes are added to the solution, for it is well-known that high ionic content leads to suppression of the stratification phenomena.[20,26]

Thin-Film Apparatus and Imaging Systems. Drainage and stratification experiments in horizontal foam films were carried out in two types of geometries: (a) a porous plate cell (see Figure 1a) and (b) a Scheludko-like cell (see schematic in Zhang and Sharma).[31] In both cases, a circular thin film with nearly plane-parallel interfaces is formed at the center of a closed cylindrical cell, and a syringe pump is used for controlling the fluid. In analogy with horizontal films within real foams, the thin film formed within the cell is always in contact with a thicker meniscus region (referred to as plateau border). To make a meaningful comparison between solutions with different surfactant and micellar concentration, we conducted experiments on films that are nearly plane-parallel and of similar initial size. The cell is placed within a closed container to minimize the effect of evaporation. The porous plate cell with hole diameter d_c = 1.0 mm was made from a porous glass fritz with pore sizes in the range of 10−15 μm. The cell geometry and the mean pore size determine the attainable capillary pressure, which is in the range from 50−4000 Pa. In the Scheludko-like cell of internal diameter d_c = 1.6 mm, liquid is slowly withdrawn from the biconcave drop to create the desired film diameter ($d_f \approx 0.6$ mm). The fluid volume is then maintained constant throughout the initial drainage process, and fluid withdrawal using the side arm induces latter transitions. Assuming perfect wetting of the inner wall of the cell holder and a small contact angle between the film and the border region, the capillary pressure in the Scheludko-type cell[28] can be estimated by[20] $P_c \approx \frac{4\gamma d_c}{d_c^2 - d_f^2}$. Here γ is the surface tension of the solution ($\gamma \approx 36$ mN/m for SDS solutions above CMC, measured using a maximum bubble pressure tensiometer designed within the laboratory), d_c and d_f are the inner diameter of the cell and the diameter of the thin film, respectively. The typical initial capillary pressure in experiments with Scheludko cells used in this study is $P_c \approx$ 50 Pa. Since the disjoining pressure becomes large at small thicknesses (as shown in Figure 1d and Figure S2a in the Supporting Information), the relatively small capillary pressure in Scheludko-like cell is not sufficient to induce further stepwise thinning, so fluid is withdrawal using the side arm to induce latter transitions. In an alternative protocol[29,45] emulated for comparison, the cell container is opened briefly to allow evaporation, which results in an increase in the capillary pressure and consequently in a step transition. The high-resolution video and images of the stratification process are captured by an imaging system that consists of a high resolution, high-speed camera (Photron FASTCAM, Mini UX100) and a precision microscope lens system (Navitar Zoom 600, with added microscope objective). The IDIOM method can be realized with a variety of light sources and cameras including commercial grade digital-SLR cameras and light sources (see Supporting Information for detailed discussion). The images are postprocessed in MATLAB R2014a with specially written codes, and the "equivalent film thickness"[28,31] is determined by using eq 1 and the reflected light intensity values for red, green, and blue (or R, G, B) channels, respectively.

ASSOCIATED CONTENT

Supporting Information

The Supporting Information is available free of charge on the ACS Publications website at DOI: 10.1021/acsnano.6b01012.

Experimental details and data (PDF)

Video of the stratification process (AVI)

AUTHOR INFORMATION

Corresponding Author

*E-mail:viveks@uic.edu.

Notes

The authors declare no competing financial interest.

DOI: 10.1021/acsnano.6b01012
ACS Nano XXXX, XXX, XXX−XXX

REFERENCES

(1) Israelachvili, J. N. *Intermolecular and Surface Forces*, 3rd ed.; Academic Press: Waltham, MA, 2011.
(2) Butt, H.-J.; Cappella, B.; Kappl, M. Force Measurements with the Atomic Force Microscope: Technique, Interpretation and Applications. *Surf. Sci. Rep.* **2005**, *59*, 1−152.
(3) Mukherjee, R.; Sharma, A. Instability, Self-Organization and Pattern Formation in Thin Soft Films. *Soft Matter* **2015**, *11*, 8717−8740.
(4) Blossey, R. *Thin Liquid Films: Dewetting and Polymer Flow*; Springer Science: Dordrecht, 2012.
(5) Craster, R. V.; Matar, O. K. Dynamics and Stability of Thin Liquid Films. *Rev. Mod. Phys.* **2009**, *81*, 1131−1198.
(6) Becker, J.; Grün, G.; Seemann, R.; Mantz, H.; Jacobs, K.; Mecke, K. R.; Blossey, R. Complex Dewetting Scenarios Captured by Thin-Film Models. *Nat. Mater.* **2003**, *2*, 59−63.
(7) Popescu, M. N.; Oshanin, G.; Dietrich, S.; Cazabat, A. Precursor Films in Wetting Phenomena. *J. Phys.: Condens. Matter* **2012**, *24*, 243102.
(8) Seemann, R.; Herminghaus, S.; Jacobs, K. Structure Formation in Thin Liquid Films. In *Thin Films of Soft Matter*, Kalliadasis, S., Thiele, U., Eds. SpringerWien: New York, 2007.
(9) Fennell Evans, D.; Wennerström, H. *The Colloidal Domain: Where Physics, Chemistry, Biology, and Technology Meet*, 2nd ed.; Wiley-VCH: New York, 1999.
(10) Ivanov, I. B. *Thin Liquid Films: Fundamentals and Applications*; CRC Press: Boca Raton, FL, 1988; Vol. *29*.
(11) Exerowa, D.; Kruglyakov, P. M. *Foam and Foam Films: Theory, Experiment, Application*; Elsevier: Amsterdam, 1997; Vol. *5*.
(12) Cantat, I.; Cohen-Addad, S.; Elias, F.; Graner, F.; Höhler, R.; Pitois, O. *Foams: Structure and Dynamics*; Oxford University Press: Oxford, 2013.
(13) Boys, C. V. *Soap Bubbles: Their Colours and the Forces Which Mold Them*; Society for Promoting Christian Knowledge: London, 1912; Vol. *542*.
(14) Mysels, K. J.; Frankel, S.; Shinoda, K. *Soap Films: Studies of Their Thinning and a Bibliography*; Pergamon Press: Oxford, 1959.
(15) Gochev, G.; Platikanov, D.; Miller, R. Chronicles of Foam Films. *Adv. Colloid Interface Sci.* **2015**, DOI: 10.1016/j.cis.2015.08.009.
(16) Derjaguin, B. V.; Churaev, N. V.; Muller, V. M. *Surface Forces*; Springer: New York, 1987.
(17) Langevin, D.; Sonin, A. A. Thinning of Soap Films. *Adv. Colloid Interface Sci.* **1994**, *51*, 1−27.
(18) Nikolov, A. D.; Wasan, D. T.; Kralchevsky, P. A.; Ivanov, I. B. Ordering and Organization in Ionic Solutions. In *Ordered Structures in Thinning Micellar Foam and Latex Films*; Ise, N., Sogami, I., Eds.; World Scientific: Singapore, 1988; pp 302−414.
(19) Kralchevski, P.; Nikolov, A.; Wasan, D. T.; Ivanov, I. Formation and Expansion of Dark Spots in Stratifying Foam Films. *Langmuir* **1990**, *6*, 1180−1189.
(20) Nikolov, A. D.; Wasan, D. T. Ordered Micelle Structuring in Thin Films Formed from Anionic Surfactant Solutions: I. Experimental. *J. Colloid Interface Sci.* **1989**, *133*, 1−12.
(21) Wasan, D. T.; Nikolov, A. D. Thin Liquid Films Containing Micelles or Nanoparticles. *Curr. Opin. Colloid Interface Sci.* **2008**, *13*, 128−133.
(22) von Klitzing, R.; Thormann, E.; Nylander, T.; Langevin, D.; Stubenrauch, C. Confinement of Linear Polymers, Surfactants, and Particles between Interfaces. *Adv. Colloid Interface Sci.* **2010**, *155*, 19−31.
(23) Oswald, P.; Pieranski, P. *Smectic and Columnar Liquid Crystals: Concepts and Physical Properties Illustrated by Experiments*; CRC Press: Boca Raton, FL, 2005.
(24) Pieranski, P.; Beliard, L.; Tournellec, J.-P.; Leoncini, X.; Furtlehner, C.; Dumoulin, H.; Riou, E.; Jouvin, B.; Fénerol, J.-P.; Palaric, P. Physics of Smectic Membranes. *Phys. A (Amsterdam, Neth.)* **1993**, *194*, 364−389.
(25) Bergeron, V. Forces and Structure in Thin Liquid Soap Films. *J. Phys.: Condens. Matter* **1999**, *11*, R215−R238.
(26) Bergeron, V.; Radke, C. J. Equilibrium Measurements of Oscillatory Disjoining Pressures in Aqueous Foam Films. *Langmuir* **1992**, *8*, 3020−3026.
(27) Bergeron, V.; Radke, C. J. Disjoining Pressure and Stratification in Asymmetric Thin-Liquid Films. *Colloid Polym. Sci.* **1995**, *273*, 165−174.
(28) Sheludko, A. Thin Liquid Films. *Adv. Colloid Interface Sci.* **1967**, *1*, 391−464.
(29) Anachkov, S. E.; Danov, K. D.; Basheva, E. S.; Kralchevsky, P. A.; Ananthapadmanabhan, K. P. Determination of the Aggregation Number and Charge of Ionic Surfactant Micelles from the Stepwise Thinning of Foam Films. *Adv. Colloid Interface Sci.* **2012**, *183*, 55−67.
(30) Patist, A.; Kanicky, J. R.; Shukla, P. K.; Shah, D. O. Importance of Micellar Kinetics in Relation to Technological Processes. *J. Colloid Interface Sci.* **2002**, *245*, 1−15.
(31) Zhang, Y.; Sharma, V. Domain Expansion Dynamics in Stratifying Foam Films: Experiments. *Soft Matter* **2015**, *11*, 4408−4417.
(32) Johonnott, E. S. Lxviii. The Black Spot in Thin Liquid Films. *Philos. Mag.* **1906**, *11*, 746−753.
(33) Sharma, V.; Crne, M.; Park, J. O.; Srinivasarao, M. Structural Origin of Circularly Polarized Iridescence in Jeweled Beetles. *Science* **2009**, *325*, 449−451.
(34) Schwaebel, T.; Menning, S.; Bunz, U. H. F. Photoscopy: Spectroscopic Information from Camera Snapshots? *Chem. Sci.* **2014**, *5*, 1422−1428.
(35) Danov, K. D.; Basheva, E. S.; Kralchevsky, P. A.; Ananthapadmanabhan, K. P.; Lips, A. The Metastable States of Foam Films Containing Electrically Charged Micelles or Particles: Experiment and Quantitative Interpretation. *Adv. Colloid Interface Sci.* **2011**, *168*, 50−70.
(36) Perrin, J. La Stratification Des Lames Liquides. *Ann. Phys. (Paris)* **1918**, *10*, 160−184.
(37) Géminard, J.-C.; Hołyst, R.; Oswald, P. Meniscus and Dislocations in Free-Standing Films of Smectic-a Liquid Crystals. *Phys. Rev. Lett.* **1997**, *78*, 1924−1927.
(38) Picano, F.; Oswald, P.; Kats, E. Disjoining Pressure and Thinning Transitions in Smectic-a Liquid Crystal Films. *Phys. Rev. E: Stat. Phys., Plasmas, Fluids, Relat. Interdiscip. Top.* **2001**, *63*, 021705.
(39) Nguyen, Z. H.; Park, C. S.; Pang, J.; Clark, N. A. Surface Energetics of Freely Suspended Fluid Molecular Monolayer and Multilayer Smectic Liquid Crystal Films. *Proc. Natl. Acad. Sci. U. S. A.* **2012**, *109*, 12873−12877.
(40) Heinig, P.; Beltran, C. M.; Langevin, D. Domain Growth Dynamics and Local Viscosity in Stratifying Foam Films. *Phys. Rev. E* **2006**, *73*, 051607−1−8.
(41) Bergeron, V.; Jimenez-Laguna, A. I.; Radke, C. J. Hole Formation and Sheeting in the Drainage of Thin Liquid Films. *Langmuir* **1992**, *8*, 3027−3032.
(42) Rosen, M. J.; Kunjappu, J. T. *Surfactants and Interfacial Phenomena*; John Wiley & Sons: Hoboken, NJ, 2012.
(43) Poskanzer, A. M.; Goodrich, F. C. Surface Viscosity of Sodium Dodecyl Sulfate Solutions with and without Added Dodecanol. *J. Phys. Chem.* **1975**, *79*, 2122−2126.
(44) Mysels, K. J. Surface Tension of Solutions of Pure Sodium Dodecyl Sulfate. *Langmuir* **1986**, *2*, 423−428.
(45) Basheva, E. S.; Kralchevsky, P. A.; Danov, K. D.; Ananthapadmanabhan, K. P.; Lips, A. The Colloid Structural Forces as a Tool for Particle Characterization and Control of Dispersion Stability. *Phys. Chem. Chem. Phys.* **2007**, *9*, 5183−5198.

DOI: 10.1021/acsnano.6b01012
ACS Nano XXXX, XXX, XXX−XXX